

Void-Supercluster Alignments

Daeseong Park and Jounghun Lee

*Department of Physics and Astronomy, FPRD, Seoul National University, Seoul 151-747,
Korea*

pds2001@astro.snu.ac.kr, jounghun@astro.snu.ac.kr

ABSTRACT

We investigate alignments between the spin axes of cosmic voids and the principal axes of nearby superclusters using the Millennium Run simulation of a Λ CDM cosmology. The concept of void spin was first introduced by Lee and Park in 2006 to quantify the tidal effect on voids from the surrounding matter distribution. Our numerical analysis reveals that the void spin axes are strongly aligned with the supercluster minor axes, but anti-aligned with the major axes, and have no correlations with the intermediate axes. We provide physical explanations to this numerical results on the basis of tidally induced correlations. It is expected that our work will provide a new insight into the characterization of the cosmic web on the largest scale.

Subject headings: cosmology:theory — large-scale structure of universe

1. INTRODUCTION

Voids stand for those regions in the universe which have extremely low density. There is still no consensus on how to define voids. In recent numerical approaches using N-body simulations, voids are often defined as regions empty of massive dark matter halos. In real observations, however, voids are usually defined as underdense regions with the mean density contrast close to -0.9 (e.g., Hoyle & Vogeley 2004), given the limitation that we cannot observe very faint galaxies. Adopting the latter definition of voids, one can say that voids are not empty of massive dark halos but have some structures in them. An interesting question is how the void structures evolve with time.

The standard picture based on the cold dark matter paradigm explains that the voids originated from the local minima of the initial density fluctuation and have become more and

more underdense via gravitational rarefaction in the subsequent evolution (Icke 1984). Recent high-resolution simulations, however, have revealed that the evolution of the void structures is more complicated than naively predicted (e.g., Gottlöber et al. 2003; Colberg et al. 2005): Not all voids remain underdense but some fraction of them actually collapse into bound halos. Although the collapse of voids may be described qualitatively as the occurrence of the clouds-in-voids in the frame of the standard excursion set theory (Sheth & van de Weygaert 2004), it has yet to be well understood under what conditions and how frequently the collapse of voids takes place.

A first suspicion goes to the tidal forces from the surrounding matter distribution (Sahni et al. 1994). As noted by Shandarin et al. (2004, 2006), the voids should be severely disturbed by the tidal influence due to the low density. Considering this possibility, a plausible scenario is that when the tidal effect on a void wins over the gravitational rarefaction, the void will become squeezed out to collapse into a bound halo. A remaining question is how to quantify the tidal effect on voids and predict its consequences.

Very recently, Lee & Park (2006, hereafter, LP06) introduced a new concept, *the void spin angular momentum*, which is defined as

$$\mathbf{J} = \frac{1}{M_V} \sum_{\alpha}^{N_V} m_{\alpha} \mathbf{r}_{\alpha} \times \mathbf{v}_{\alpha}, \quad (1)$$

where N_v is the total number of halos belonging to a void, m_{α} , \mathbf{r}_{α} , and \mathbf{v}_{α} are the mass, the position, and the velocity of the α -th halo belonging to a void and $M_V \equiv \sum_{\alpha}^{N_V} m_{\alpha}$. Here the positions and the velocities of the void halos are measured relative to the center of mass of the void halos.

As mentioned by LP06, although the quantity defined in equation (1) is not a real spin angular momentum since voids are not bound system, the concept of void spin turned out to be a very effective measure of the tidal effect from the surrounding matter. To show that the void spin angular momentum is tidally induced, LP06 measured the spatial correlations between the spin axes of neighboring voids analyzing numerical data from high-resolution simulation, and found that the numerical results are in excellent agreement with the analytic predictions based on tidally generated correlations.

If the void spin angular momentum is really induced by the tidal effect from the surrounding matter, then there should exist correlations not only between the spin axes of neighboring voids but also between the spin axes of voids and the neighboring matter distribution. This cross correlation, if found to exist, should be a more direct indication of the tidal effect on voids from the surrounding matter.

Our goal here is to measure the cross-correlations between the void-spin axes and the

axes of the neighboring superclusters using numerical data from high-resolution simulations and to explain it physically. The superclusters are considered as the counterparts of voids since they are the largest bound structures, comparable to voids in size.

The outline of this paper is summarized as follows. In §2, the numerical data are analyzed and the signals of void-supercluster alignments are detected. In §3, analytic model for the void-supercluster alignments is derived and compared with the numerical results. In §4, the implications and caveats of our work are discussed, and a final conclusion is drawn.

2. NUMERICAL RESULTS

2.1. Measurements of Void Spins

We analyzed the halo catalog extracted from the Millennium Run simulation (Springel et al. 2005), which is now available at <http://www.mpa-garching.mpg.de/millennium>. The simulation is of a flat Λ CDM universe for which the values of the key parameters are given as $(\Omega_m, \sigma_8, h, n_s) = (0.25, 0.9, 0.73, 1)$ where Ω_m , σ_8 , h and n_s represent the matter density parameter, the rms density fluctuation on the top-hat scale of $8h^{-1}$ Mpc, the dimensionless Hubble parameter and the slope of the primordial power spectrum.

For our analysis, we exclude those halos from the Millennium Run catalog which have too low particle numbers, as those low-particle number halos are just poorly sampled, heavily affected by noise (V. Springel in private communication). Technically, we set the cut-off particle number at 50, a minimum particle number for defining a halo density profile.

In accordance with the void-finder algorithm proposed by Hoyle & Vogeley (2002, hereafter, HV02) to the Millennium Run halo catalog, we take the following steps to identify voids: First, we classify the halos according to the wall/field criterion, given as $l = \bar{d}_3 + 3\sigma/2$, where \bar{d}_3 is the average distance to the third nearest neighbor and σ is its standard deviation. For the Millennium Run halos, the criterion distance is found to be $l = 2.78h^{-1}$ Mpc. Note that this value is slightly higher than the value $l = 2.44h^{-1}$ Mpc used in our previous work (Lee & Park 2006). It is because in our previous work the voids were identified not from the halo catalog but from the galaxy catalog. Second, we place the wall halos on cubic grid cells each of which has a linear size of l , counting the number of halos in each cell. Third, increasing the radii of empty spheres from the center of all empty grid cells till each of them include three wall halos on the surface, we determine the largest possible empty spheres.

Finally, we detect voids by categorizing the overlapping empty spheres whose radii are greater than the minimum size threshold. The minimum void size are set at $6h^{-1}$ Mpc

which was found through statistical significance test in our previous work (Lee & Park 2006). A total 20291 voids are identified in the $z=0$ catalog, among which only 6430 voids are found to have more than 30 halos. The mean density contrast ($\bar{\delta}_v$) and the mean effective Eulerian radius (\bar{R}_E) of these 6430 voids are found to be $\bar{\delta}_v = -0.9$ and $\bar{R}_E = 12.22h^{-1}\text{Mpc}$, respectively.

Considering only these large voids with more than 30 halos, we calculate the spin angular momentum by equation (1). It is worth mentioning here that the direction of the void spin angular momentum might depend on the cut-off particle number for the halo selection. In our analysis, we include only those halos in the Millennium Run halo catalog which contain more than 50 particles. One may suspect that a different cut-off particle number might yield different directions of the void spins.

To examine how the void spin angular momentum depends on the cut-off particle number, we calculate a second angular momentum \mathbf{J}' for each of the 6430 voids, taking all halos inside the void with more than 30 particles, and calculate the cosines of the angles, ψ , between \mathbf{J} and \mathbf{J}' as

$$\cos \psi \equiv \frac{|\mathbf{J} \cdot \mathbf{J}'|}{|\mathbf{J}||\mathbf{J}'|}. \quad (2)$$

Figure 1 plots the probability distribution of $\cos \psi$ as histogram with the Poisson errors. The horizontal line corresponds to the case of no correlation. As can be seen, the two angular momentum vectors are very strongly aligned. It indicates that excluding those halos with lower particle number will not affect the void spin angular momentum significantly.

2.2. Measurements of Supercluster Principal Axes

A next task is to identify superclusters from the Millennium Run halo catalog. Following the common method (e.g., Wray et al. 2006), we define a supercluster as a cluster of clusters, and identify superclusters with the help of the friends-of-friends algorithm (FOF). The cluster halos are selected as those halos whose mass exceeds a typical poor cluster mass, M_c . As in Wray et al. (2006), we set the value of M_c at $1.75 \times 10^{13}h^{-1}M_\odot$.

Before applying the FOF algorithm to the Millennium Run halo catalog, one has to determine a linking length for the supercluster identification. To find an optimal linking length, L , we perform a statistical significance test by generate 100 random Poisson samples of clusters which have the same number density in the same the box size as the Millennium halo catalog but having no clustering effect. The statistical significance of a supercluster can be estimated as $P(L) = 1 - N_{po}(L)/N_{sc}(L)$, where $N_{po}(L)$ and $N_{sc}(L)$ are the numbers of superclusters found in the random samples and in the Millennium Run simulation data at a

linking length L , respectively.(Basilakos et al. 2006).

Figure 2 plots the statistical significance $P(L)$, which reveals that around $L = 6h^{-1}$ Mpc the statistical significance of finding a supercluster reaches 99% confidence level. Therefore, we set the linking length for the FOF algorithm at $L = 6h^{-1}$ Mpc which corresponds to the linkage parameter $b = 0.35$.

A total of 4014 superclusters are found. Among them, a total of 382 superclusters are found to consist of more than 5 members. The mean mass of these 382 superclusters are found to be $\bar{M}_s = 4.2 \times 10^{14}h^{-1}M_\odot$. Using these superclusters, we measured the inertia momentum tensor of each supercluster. Rotating the system into the principal axis frame, we find the three eigenvectors of the inertia momentum tensor of each supercluster.

2.3. Alignments between Void Spin and Supercluster Principal Axes

Now that the spin axes of voids and the principal axes of the superclusters are all determined, we calculate the squares of the cosines of the angles between the the void spin axes and the three axes of the superclusters as a function of the separation distance, r . Let $\hat{\mathbf{y}}^\alpha, \hat{\mathbf{y}}^\beta, \hat{\mathbf{y}}^\gamma$ be the three unit eigenvectors of the supercluster inertia momentum tensor, which represent the supercluster major, intermediate, and minor axes, respectively. Basically, we calculate the following three correlation functions using the selected void-supercluster pairs:

$$\omega^\alpha(r) \equiv \langle |\hat{\mathbf{J}} \cdot \hat{\mathbf{y}}^\alpha|^2 \rangle(r) - \frac{1}{3}, \quad (3)$$

$$\omega^\beta(r) \equiv \langle |\hat{\mathbf{J}} \cdot \hat{\mathbf{y}}^\beta|^2 \rangle(r) - \frac{1}{3}, \quad (4)$$

$$\omega^\gamma(r) \equiv \langle |\hat{\mathbf{J}} \cdot \hat{\mathbf{y}}^\gamma|^2 \rangle(r) - \frac{1}{3}. \quad (5)$$

If there is no alignment, then these cross-correlation function will be just zero.

To examine how these void-supercluster cross correlations depend on the linking length, we repeat the whole process using different values of L . The three cross-correlations functions between the void spin axes and the supercluster major (ω^α), intermediate (ω^β), and minor axes (ω^γ) for the fives different cases of the linking lengths are plotted in Figs. 3, 4 and 5. As can be seen, for those values of L that corresponds to higher than 90% confidence levels (i.e., $L \leq 7h^{-1}$ Mpc), there are clear consistent anti-alignment and alignment signals between the void spin axes and the supercluster major and the minor axes, respectively, within a distance of $30h^{-1}$ Mpc, and there is consistently no alignment signal with the supercluster intermediate axes.

We provide physical explanations to this phenomena in §3 within the analytic framework proposed originally by Lee & Pen (2001).

3. ANALYTIC PREDICTION

3.1. Review of Spin-Shear and Direction-Shear Correlations

According to the Lee-Pen formalism based on the linear tidal torque theory (Doroshkevich 1970; White 1984), the unit spin vector $\hat{\mathbf{J}} \equiv (\hat{J}_i)$ of a bound halo is correlated with the unit traceless tidal shear tensor $\hat{\mathbf{T}} \equiv (\hat{T}_{ij})$ as

$$\langle \hat{J}_i \hat{J}_j | \hat{\mathbf{T}} \rangle = \frac{1+a}{3} \delta_{ij} - a \hat{T}_{ik}(\mathbf{x}) \hat{T}_{kj}(\mathbf{x}), \quad (6)$$

where a is the spin-shear correlation parameter in the range of $[0, 3/5]$. It represents the strength of the correlation between $\hat{\mathbf{J}}$ and $\hat{\mathbf{T}}$: If $a = 3/5$, the correlation is strongest. If $a = 0$, there is no correlation. Here, the unit tidal tensor $\hat{\mathbf{T}}$ is intrinsic and local, defined at the halo position, \mathbf{x} .

Lee & Pen (2001) also suggested the following formula for the correlation between the direction vector to the nearest neighbor $\hat{\mathbf{y}} \equiv (\hat{y}_i)$ with the unit traceless tensor $\hat{\mathbf{T}}$ as

$$\langle \hat{y}_i \hat{y}_j | \hat{\mathbf{T}} \rangle = \frac{1-b}{3} \delta_{ij} + b \hat{T}_{ik}(\mathbf{x}) \hat{T}_{kj}(\mathbf{x}), \quad (7)$$

Here the parameter, b in the range of $[-1, 1]$ represents the strength of the correlation between $\hat{\mathbf{y}}$ and $\hat{\mathbf{T}}$. Note the difference in the range between the two correlation parameters, a and b . The maximum value of b is 1 while that of a is $3/5$, less than unity. It reflects the fact that a perfect alignment is allowed between $\hat{\mathbf{y}}$ and $\hat{\mathbf{T}}$ but not between $\hat{\mathbf{J}}$ and $\hat{\mathbf{T}}$.

Anyway, a crucial implication of equations (6) and (7) is that the spin axes of halos should be closely correlated with the directional geometry of the nearby halo distribution since $\hat{\mathbf{J}}$ and $\hat{\mathbf{y}}$ are both correlated with the tidal field. In §3.2, we extrapolate the validity of equations (6) and (7) which hold good for halos to the voids and superclusters.

3.2. Modeling Void-Supercluster Alignments

LP06 have already extrapolated the validity of equation (6) to unbound voids, assuming that the spin-shear correlation parameter a has the maximum value of $3/5$ for the case of

voids whose spin is defined as (1):

$$\langle \hat{J}_i \hat{J}_j | \hat{\mathbf{T}} \rangle = \frac{8}{15} \delta_{ij} - \frac{3}{5} \hat{T}_{ik}(\mathbf{x}_v) \hat{T}_{kj}(\mathbf{x}_v), \quad (8)$$

where $\hat{\mathbf{T}}$ is now defined at the void center, \mathbf{x}_v .

Now, we attempt to extrapolate the validity of equation (7) to the alignments between the void spin axes and the supercluster principal axes. The superclusters are conspicuously elongated along local filaments where the dark matter are preferentially located. The nearest neighbors are most likely to be found in the direction along the supercluster major axes. But, the filaments are one dimensional structure, collapsed along the major and the intermediate principal axes of the local tidal tensors. Thus, the direction of local filaments (i.e., the supercluster major axes) are in fact anti-aligned with the tidal tensor major axes, and aligned with the tidal tensor minor axes.

Using the above logic, we assume the following:

- For the direction of the supercluster major axis, $\hat{\mathbf{y}}^\alpha$, the direction-shear correlation parameter b has the minimum value of -1 :

$$\langle \hat{y}_i^\alpha \hat{y}_j^\alpha | \hat{\mathbf{T}} \rangle = \frac{2}{3} \delta_{ij} - \hat{T}_{ik}(\mathbf{x}_s) \hat{T}_{kj}(\mathbf{x}_s). \quad (9)$$

- For the direction of the supercluster intermediate axis, $\hat{\mathbf{y}}^\beta$, the direction-shear correlation parameter b has the value of 0:

$$\langle \hat{y}_i^\beta \hat{y}_j^\beta | \hat{\mathbf{T}} \rangle = \frac{1}{3} \delta_{ij}, \quad (10)$$

- For the direction of the supercluster minor axis, $\hat{\mathbf{y}}^\gamma$, the parameter b has the maximum value of 1:

$$\langle \hat{y}_i^\gamma \hat{y}_j^\gamma | \hat{\mathbf{T}} \rangle = \hat{T}_{ik}(\mathbf{x}_s) \hat{T}_{kj}(\mathbf{x}_s), \quad (11)$$

Note that in equations (9)-(11), the unit tidal tensor is defined at the supercluster center, \mathbf{x}_s .

Using equations (8)-(11), one can derive analytically the three correlation functions, ω^α , ω^β and ω^γ , defined in §2.. In this derivation, the key part is to calculate the four point shear correlation, $\langle \hat{T}(\mathbf{x}_v) \hat{T}(\mathbf{x}_v) \hat{T}(\mathbf{x}_s) \hat{T}(\mathbf{x}_s) \rangle$. Lee & Pen (2001) calculated this quantity for the case that the two unit tidal tensors are defined at the same halo position but smoothed on two different scales. What they found is that it is approximated as the density auto-correlation (see Appendix I in Lee & Pen 2001). In our case, the two unit tidal tensors are

not defined at the same position but at two different positions, the void and the supercluster centers. Therefore, the four-point shear correlation would not be approximated as the density autocorrelation. Instead, it may be approximated as the density two-point correlation, just like the void spin-spin correlation function (Lee & Park 2006).

Hence, using the same approximation used in (Lee & Park 2006) but considering the fact that the maximum value of the correlation parameter b is different from that of a , we find that the void-supercluster alignments can be approximated as

$$\omega^\alpha(r) \approx -\frac{1}{10} \frac{\xi_R^2(r)}{\xi_R^2(0)}, \quad (12)$$

$$\omega^\beta(r) \approx 0, \quad (13)$$

$$\omega^\gamma(r) \approx \frac{1}{10} \frac{\xi_R^2(r)}{\xi_R^2(0)}, \quad (14)$$

where $r \equiv |\mathbf{x}_v - \mathbf{x}_s|$. Here ξ_R is the two point correlation function of the density field on the smoothing scale of R . For the void-supercluster alignments, the smoothing scale should be a minimum Lagrangian radius enclosing a void-supercluster pair. Since the separation distance r cannot decrease below the sum of the supercluster radius and the void diameter in Lagrangian space, the smoothing scale may be written as

$$R = R_s + 2R_v, \quad (15)$$

where R_s and R_v represent the effective radii of a supercluster and a void, respectively.

For the comparison with the numerical results, we relate the Lagrangian supercluster and void radii to the observables given in §2:

$$\bar{R}_s \equiv \left(\frac{3\bar{M}_s}{4\pi\bar{\rho}} \right)^{1/3}, \quad \bar{R}_v \equiv (1 + \bar{\delta}_v)^{1/3} \bar{R}_E, \quad (16)$$

where $\bar{\rho}$ is the mean mass density of the universe.

Equations (12), (13) and (14) are plotted in Figs. 6, 7 and 8, respectively, where the numerical results (with $L = 6h^{-1}\text{Mpc}$) derived in §2.3 are also plotted as solid dots with Poissonian errors. For the analytic results, we use the transfer function of the initial power spectrum given by Bardeen et al. (1986) with the cosmological parameters set at the values used in the Millennium Run simulations. And, the shape parameter, Γ is approximated as $\Gamma = \Omega_m h$ (V. Springel in private communication). As can be obviously seen, the analytic approximations work very well. The excellent agreements between the analytical and the numerical results imply that the void-supercluster alignments are indeed generated by the tidal interactions between the voids and the superclusters.

4. DISCUSSION AND CONCLUSION

We have investigated correlations in spatial orientations between voids and their neighbor superclusters using the Millennium Run simulation of a concordance cosmology. Adopting the concept of void spin proposed by Lee & Park (2006), we have found for the first time that the void spin axes are very strongly correlated with the supercluster minor axes within the separation distance of $30h^{-1}\text{Mpc}$. Testing how the result depend on the choice of void and supercluster definition, we have found that our result is quite solid.

To this numerical phenomena has a physical explanation been provided based on tidally generated correlations. Under the assumption that the neighboring superclusters are representative of the filamentary surrounding matter which wrap and exert tidal forces on the voids, we have derived an analytic formula for the alignments between the void spin axes and the supercluster minor axes. The analytic prediction has turned out to agree with the numerical result very well.

However, it is worth discussing a caveat which the success of our work is subject to. This caveat lies in the fact that there is no consensus on how to define voids and superclusters, unlike the case of halo-defining. Using different algorithms could produce different results for correlations between voids and superclusters. Although we have shown here that the void-supercluster alignments do not strongly depend on the linking length of the FOF algorithm and the cut-off mass of the void halos, it will definitely necessary to compare between different methods for the void and supercluster identifications in the future.

Together with our previous work on the void spin-spin correlation (Lee & Park 2006), this new result supports the scenario that the voids originate from the initial regions where the tidal effect becomes maximum. In addition, this new result on the void-supercluster alignments demonstrate more directly how the largest scale structure and voids are connected in a cosmic web through tidal influences.

A final conclusion is that our work will provide a new clue to describing the void-supercluster network in the cosmic web and leads us to have a deeper insight into the formation and evolution of the large scale structure of the universe.

The Millennium Run simulation used in this paper was carried out by the Virgo Supercomputing Consortium at the Computing Centre of the Max-Planck Society in Garching. We thank V. Springel and G. Lemson for plenty of helps. This work is supported by the research grant No. R01-2005-000-10610-0 from the Basic Research Program of the Korea Science and Engineering Foundation.

REFERENCES

- Bardeen, J.M., Bond, J.R., Kaiser, N., & Szalay, A.S. 1986, *ApJ*, 304, 15
- Basilakos, S., Plionis, M., Yepes, G., Gottlober, S., Turchaninov, V. 2005, *MNRAS*, 365, 539
- Colberg J. M., Sheth R. K., Diaferio A., Gao L., & Yoshida N. 2005, *MNRAS*, 360, 216
- Doroshkevich, A. G. 1970, *astrofizika*, 6, 581
- El-Ad, H., & Piran, T. 1997, *ApJ*, 491, 421
- Gottlöber, S., Lokas, E. L., Klypin, A., & Hoffman, Y. 2003, *MNRAS*, 344, 715
- Hoyle, F., & Vogeley, M. S. 2002, *ApJ*, 566, 641
- Hoyle, F., & Vogeley, M. S. 2004, *ApJ*, 607, 751
- Icke V. 1984, *MNRAS*, 206,
- Lee, J. & Park, D. 2006, *ApJ*, 652, 1
- Park, D. & Lee, J. 2007, submitted to *Phys. Rev. Lett.*
- Lee, J. & Pen, U. L. 2001, *ApJ*, 555, 106
- Sahni, V., Sathyaprakah, B. S., & Shandarin, S. F. 1994, *ApJ*, 431, 20
- Shandarin, S. F., Sheth, J., & Sahni, V. 2004, *MNRAS*, 353, 517
- Shandarin, S., Feldman, H. A., Heitmann, K., & Habib, S. 2006, *MNRAS*, 367, 1629
- Sheth, R. K., & van de Weygaert, R. 2004, *MNRAS*, 350, 517
- Springel, V. et al. 2005, *Nature*, 435, 629
- Wray, J. J., Bahcall, N. A., Bode, P., Boettiger, C., Hopkins, P. F. 2006, *ApJ*, 652, 907
- White, S. D. M. 1984, *ApJ*, 286, 38

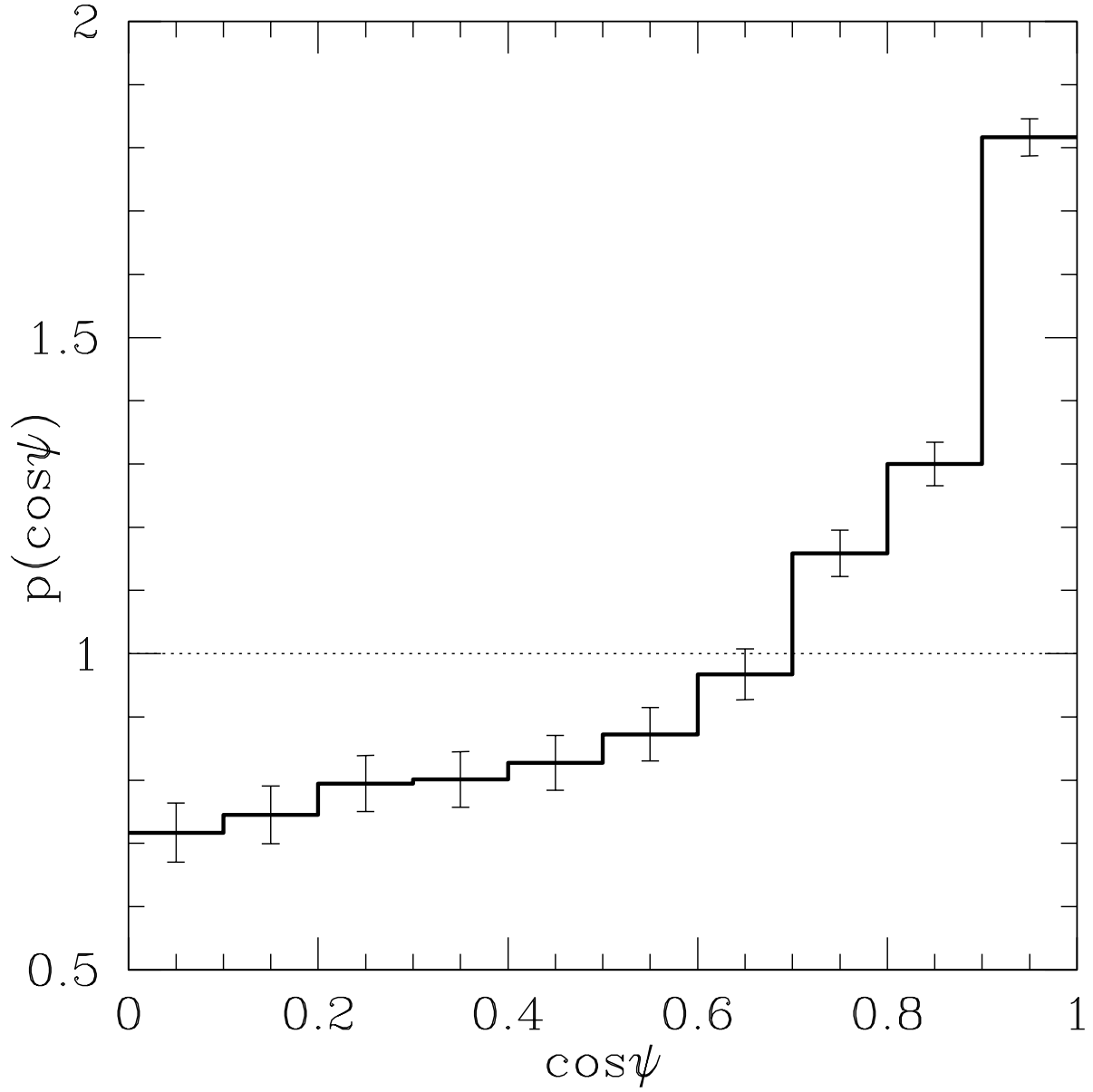


Fig. 1.— The probability density distribution of the cosines of the angles between \mathbf{J} and \mathbf{J}' .

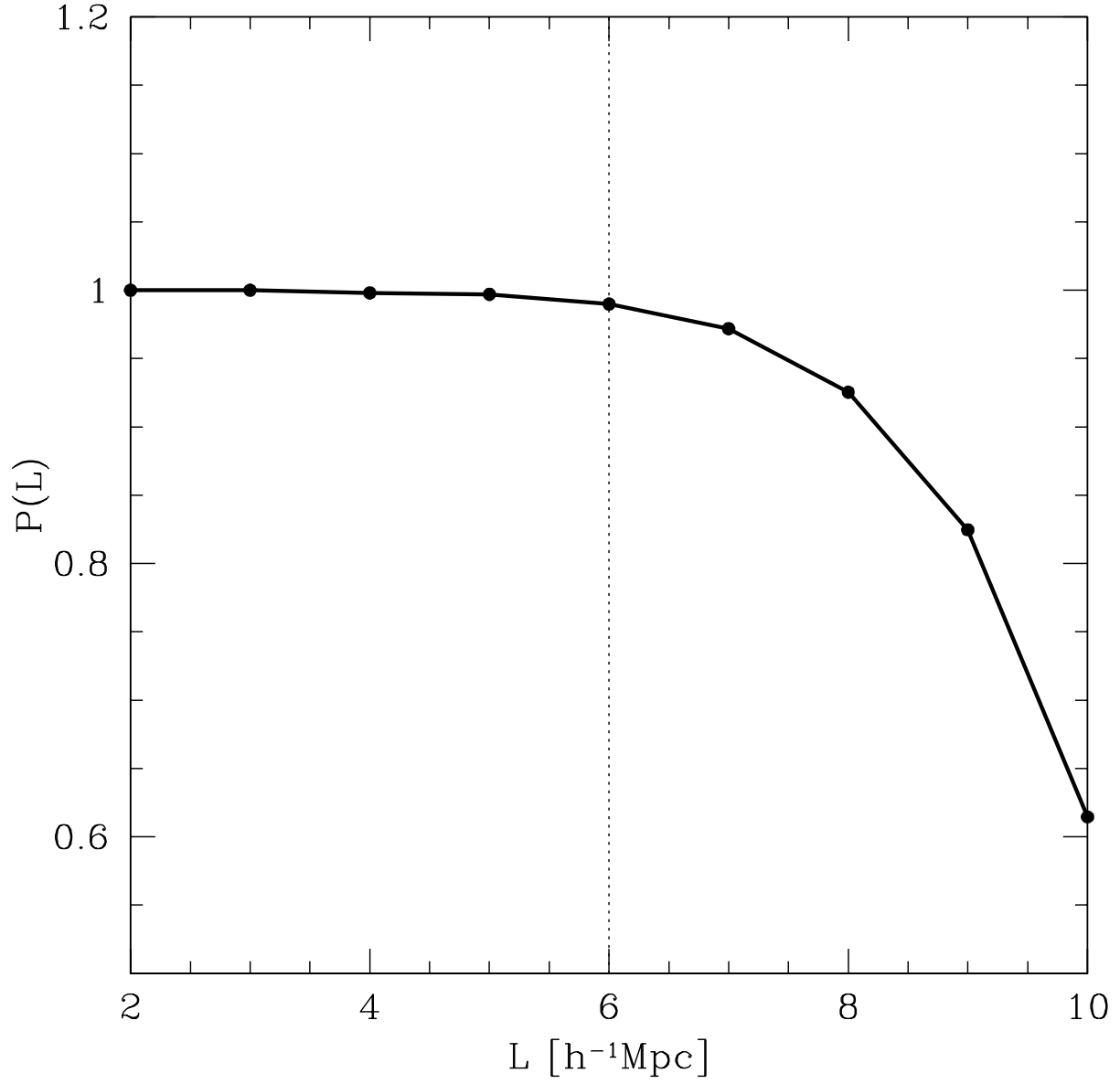


Fig. 2.— The statistical significance of the linking length for the FOF algorithm to find superclusters in the Millennium Run halo catalog.

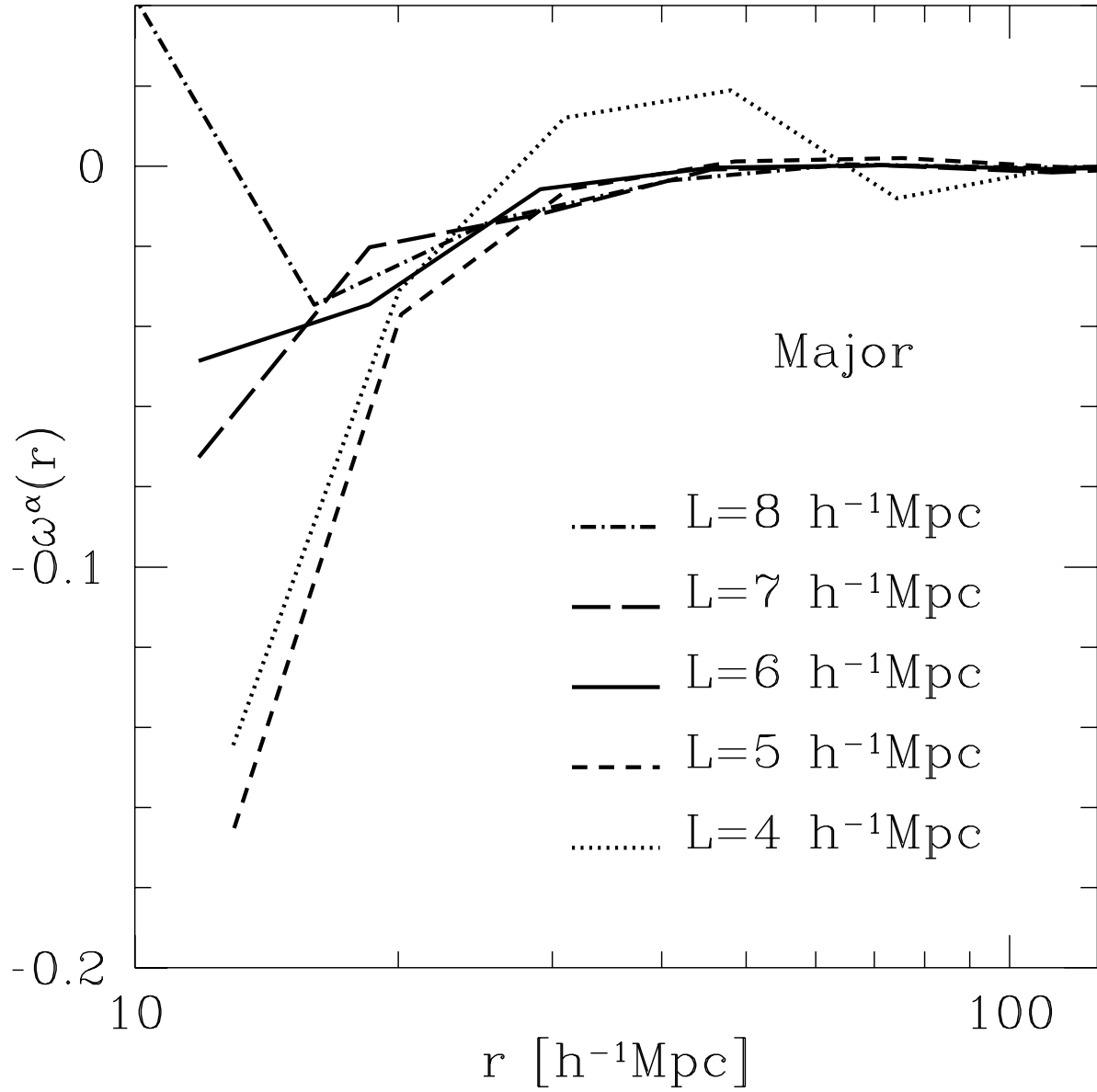


Fig. 3.— Numerical result of the cross-correlation between the void spin axes and the major axes of the neighboring superclusters as a function of separation distance for the five different cases of the linking length, L .

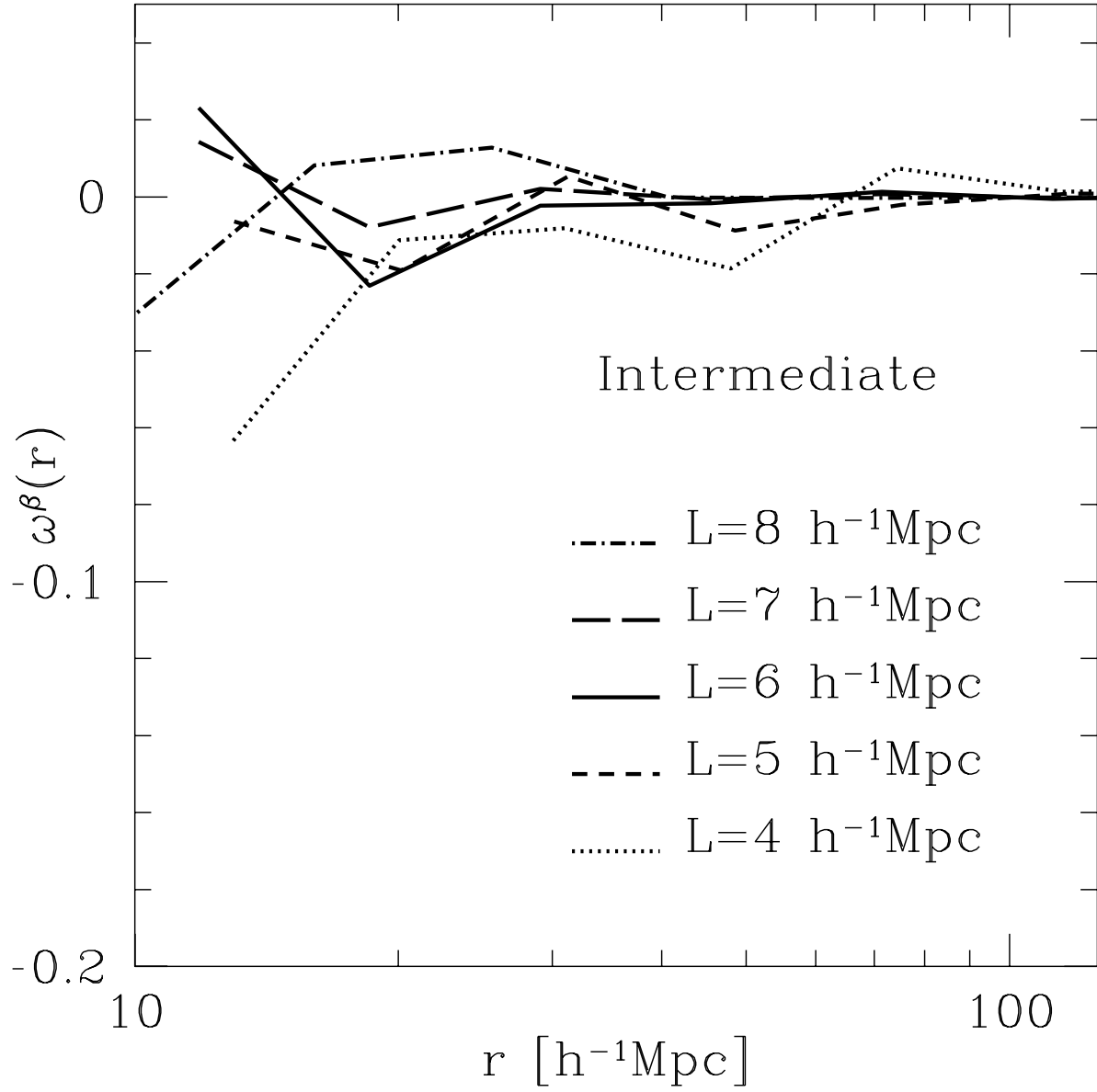


Fig. 4.— Same as Figure 6 but with the supercluster intermediate axes.

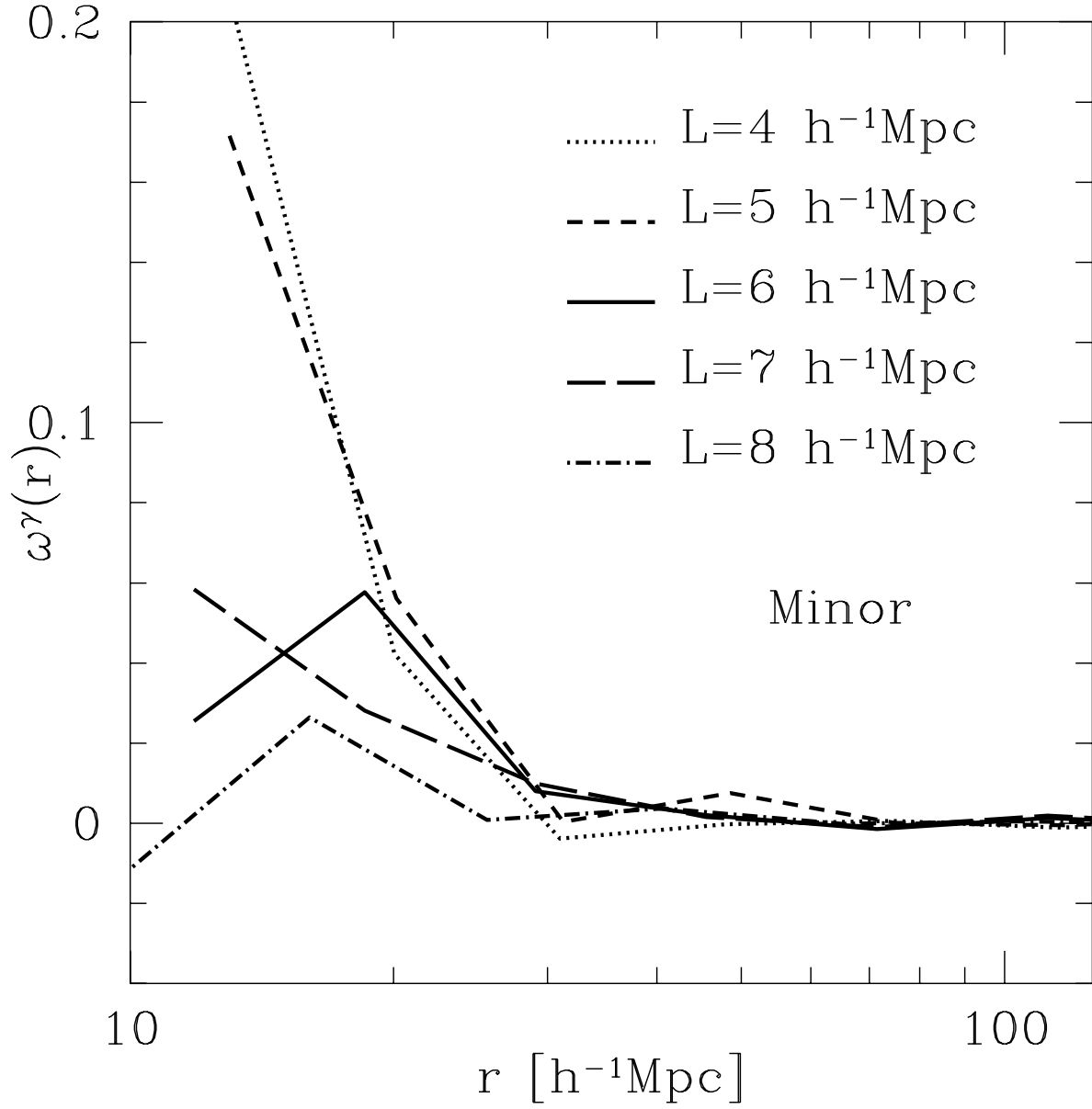


Fig. 5.— Same as Figure 6 but with the supercluster minor axes.

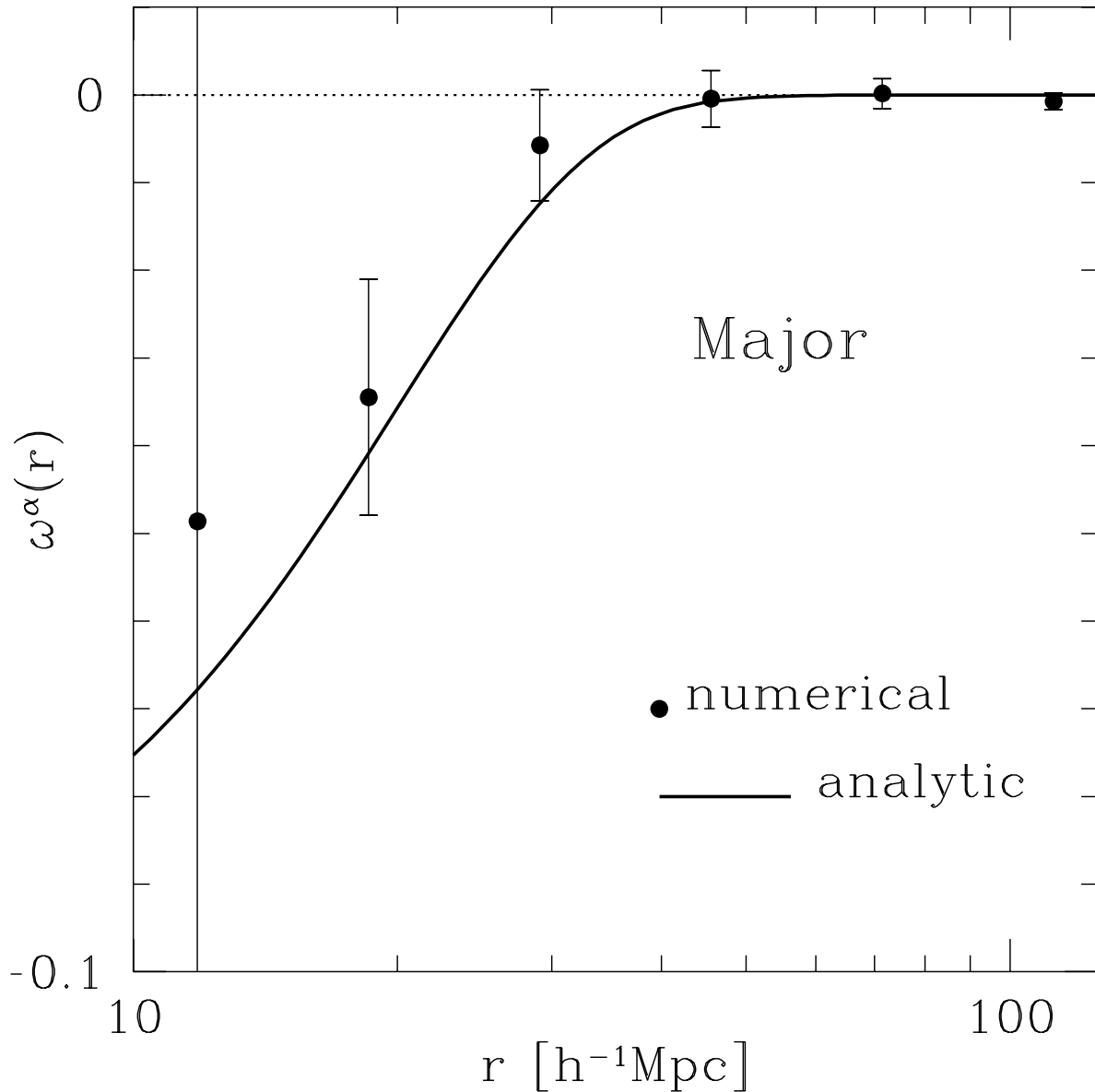


Fig. 6.— Comparison of the analytic cross-correlation between the void spin axes and the major axes of the neighboring superclusters (solid line) with the numerical result from the Millennium Run simulation (dots). The linking length for the numerical result is set at 6^{-1}Mpc which corresponds to the 99% confidence level for the supercluster identification using the FOF algorithm. The errors represent the standard deviation for the case of no alignment. The horizontal line corresponds to the case of no alignment

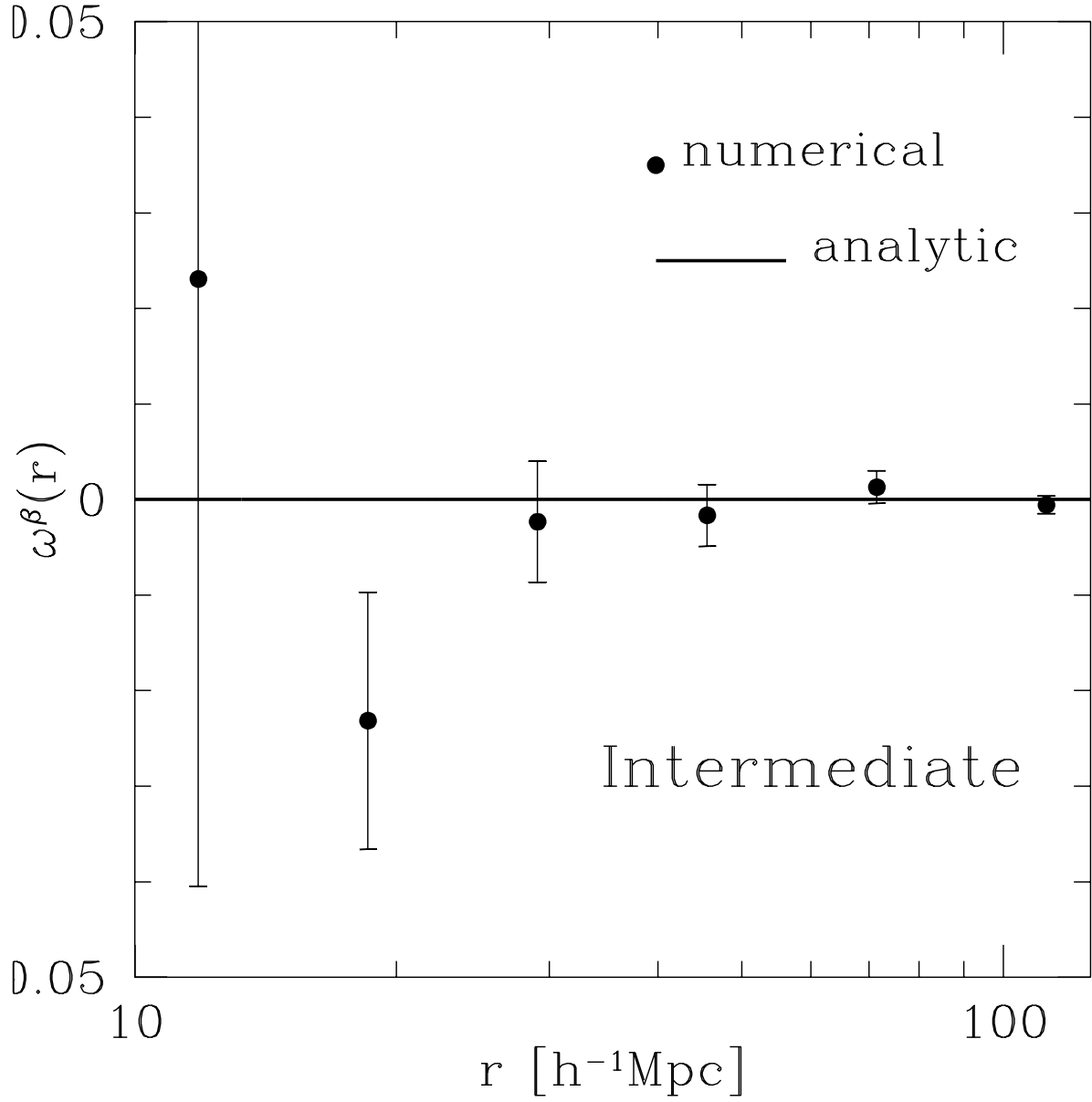


Fig. 7.— Same as Figure 6 but with the supercluster intermediate axes.

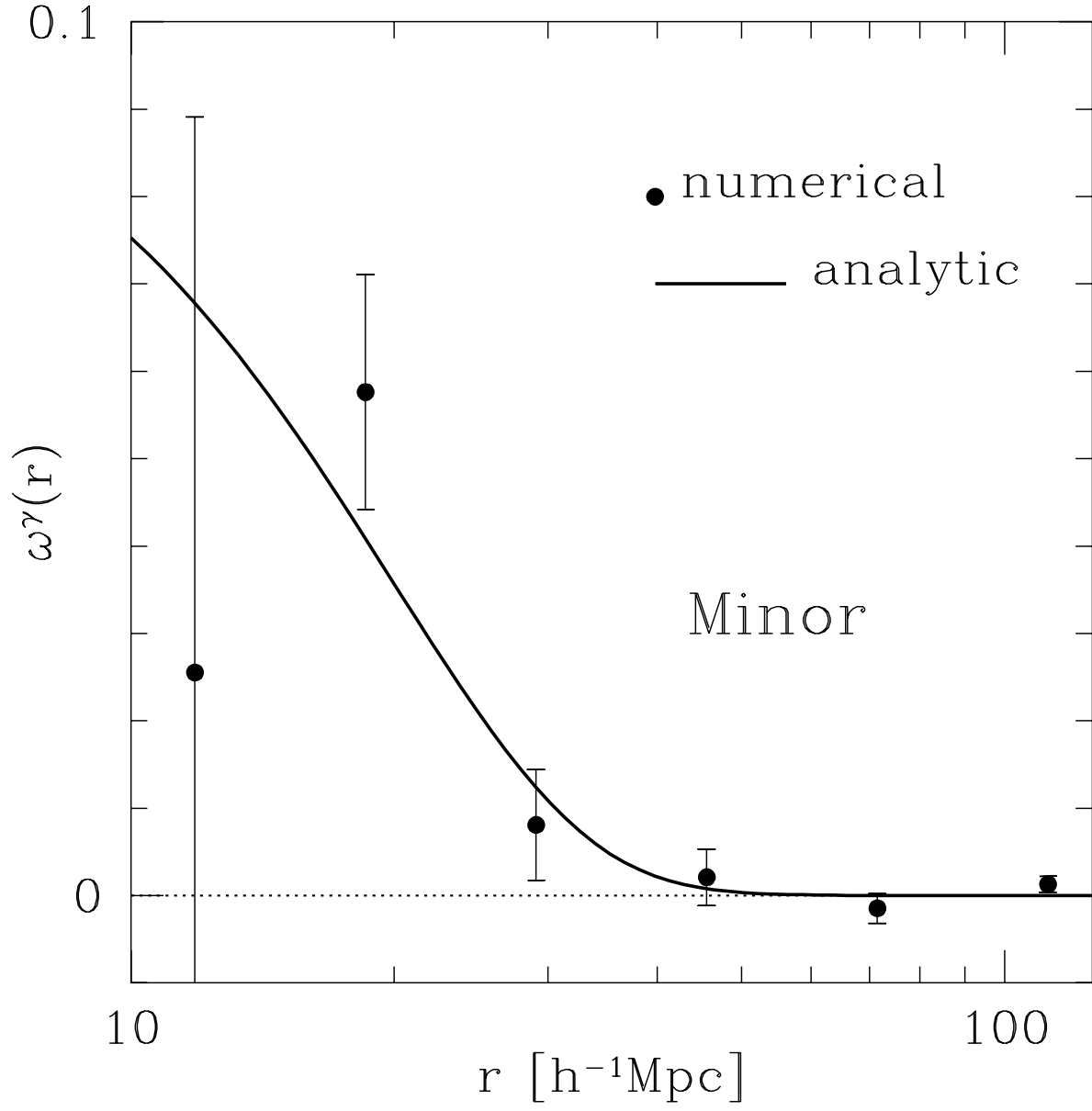


Fig. 8.— Same as Figure 6 but with the supercluster minor axes.